INTERNATIONAL JOURNAL OF INNOVATIVE RESEARCH & DEVELOPMENT

ISSN 2278 – 0211 (Online)

Lung Tissue Classification for Lung Disease Diagnosis

V. Lakshmi
Department of Electronics and Communication Engineering
Sri Vidya College of Engineering and Technology, Virudhunagar, Tamilnadu, India
P. Krisnaveni
Department of Electronics and Communication Engineering
Sri Vidya College of Engineering and Technology, Virudhunagar, Tamilnadu, India

Abstract:
In this paper, a new method for Lung tissue Classification using Patch adaptive sparse approximation with two feature descriptors is proposed. Operator assisted classification methods are impractical for large amounts of data .High resolution Computed Tomography images contain a noise caused by operator performance which can lead to serious inaccuracies in classification. We design two new feature descriptors for higher feature descriptiveness, namely the rotation-invariant Gabor-local binary patterns (RGLBP) texture descriptor and multi-coordinate histogram of oriented gradients (MCHOG) gradient descriptor. Each image patch is then labeled based on its feature approximation from reference image patches. Decision making was performed in two steps, Feature extraction using the two feature descriptors ii) classification using Patch adaptive sparse approximation.

Key words: *Adaptive, gradient, reference, texture*

1. Introduction

The interstitial lung disease (ILD) represents a group of more than 150 disorders of the lung parenchyma[1]. Most of these cause progressive scarring of lung
tissues and eventually affect breathing. Determining the specific type of disorder is important for treatment, and in conjunction with other methods, such as blood tests and pulmonary function tests, imaging scans are

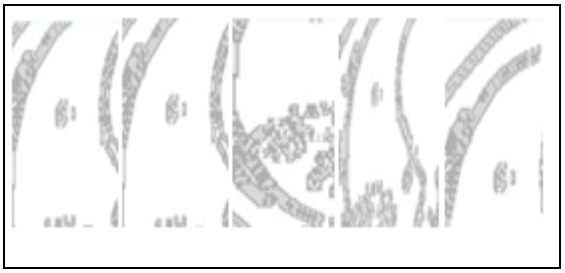

Figure 1; Tissue Patterns
From Left To Right: Normal, Emphysema, Ground Glass, Fibrosis, And Micro nodules

Often used for accurate diagnosis. In particular, HRCT imaging is quickly becoming the standard practice with its high imaging quality. Different ILDs normally exhibit different combinations of tissue patterns on HRCT images, and differentiating the tissue patterns is critical to identify the actual type of ILD. However, interpreting the HRCT images for lung diseases is challenging even for trained radiologists. Patients also have different physical conditions and medical histories; hence even those with the same type of ILD could display quite different tissue patterns. As a consequence, manual interpretation of the images could be error prone, especially when the radiologists are under heavy workload with short time frames. It is thus suggested that an automatic system for differentiating the tissue patterns would be useful to provide initial screening or second opinions. In this study, we focus on classification of five categories of lung tissues on HRCT images—normal, emphysema, groundglass, fibrosis, and micronodules, which are highly prevalent among the main type of ILDs

Examples of these tissue patterns are shown in Figure. 1. It can be seen that while in general there are perceivable differences between the different categories, the visual distinctions between different categories are sometimes subtle, and the pattern variations within the same tissue category are rather obvious. Therefore, it is quite challenging to design a robust method for automatic classification, accommodating both low inter-class distinctions and high intra-class variations.

2. Related Work

Image classification is normally performed in two stages: feature extraction for encoding the image features as feature descriptors, and labeling of image categories using supervised approaches. Being an active research field for a long time, most of the image classification techniques have been applied to a wide range of imaging problems, including the lung CT images. We will thus review mainly the recent works on lung CT images to cover the popular methodologies, and only include studies from other imaging domains if the proposed methods are not normally used for lung studies [1]. Zhengyi Yang, Jeiran Choupan explained that the tissue Classification for PET/MRI Attenuation Correction using Conditional Random Field and Image Fusion to the inclusion of PET data improved the classifier's performance in terms of classification accuracy. But the feature set used in classifiers plays a critical role and finding the relevant features to the learning task is often too expensive to explicitly enumerate and compare all the candidate feature subsets [2]. S. Sivakumar, C. Chandrasekar explained that Detection of lung nodules is a challenging task since the modules are commonly attached to the blood vessels. This paper aims to develop an efficient lung nodule detection scheme by performing nodule segmentation through fuzzy based clustering models; classification by using a machine learning technique called Support Vector Machine (SVM). This methodology uses three different types of kernels among these RBF kernel gives better class performance. The advantage of this method is better classification. Demerit is even though the FCM algorithm yields good results for segmenting noise free images, it fails to segment images corrupted by noise [3]. Anam Tariq, M. Usman Akram proposed that a computerized system for lung nodule detection in CT scan images. The automated system consist of two stages1.feature extraction 2.classifiation.The segmentation process will result in separating lung tissue from rest of the image and only the lung tissues under examination are considered as candidate regions for detecting malignant nodules in lung portion. Advantage of this method is accuracy. Demerit of this method is low feature extraction[4].Adrien Depeursinge, Dimitri Van de Ville proposed that near-affine-invariant texture descriptors derived from isotropic wavelet frames for the characterization of lung tissue patterns in high-resolution computed tomography HRCT imaging to provide classification accuracy of 76.9%.But 3-D WTs are not appropriate for analyzing HRCT image series because filtering along the *z*-axis with a very low axial resolution (20 to 50 slices with 10-mm distance) leads to coarse blurring of the relevant information[5].Ulas bagsi ,Jianhua yao presents a novel computer-assisted detection (CAD) system for automatically detecting and precisely quantifying abnormal nodular branching opacities in chest computed tomography (CT), termed tree in bud(TIB) opacities by radiology literature to accurate lung tissue classification but it takes more time for computational[6].V.Kumar, S.Jeyanthi gives information about automated vessel tree segmentation Algorithm. This method utilizes Fuzzy Support Vector Machine (SVM) classifier which improves traditional SVM by adding fuzzy membership to training sample to indicate degree of membership of this sample to different class. Consequently it reduces noises and outliers in data and enhances performance and accuracy of SVM but feature extraction is low [7]. Qi song, Milan Sonka presents an automatic algorithm for pathological lung CT image segmentation that uses a graph search driven by a cost function combining the intensity, gradient, boundary smoothness, and the rib information. They use KNN classifier for feature extraction. This method has better performance because image intensity, and image gradient are combined into the cost function for graph search algorithm .But this method have high computational time [8]. Jianhua Yao, Andrew Dwyer suggested that to develop and test a computer-assisted detection method for identification and measurement of pulmonary abnormalities on chest CT in cases of infection. This method developed could be a potentially useful tool for classifying and quantifying pulmonary infectious disease on CT. Forty Chest CTs were studied using texture analysis and support vector machine (SVM) classification to differentiate normal from abnormal lung regions on CT. This method has high texture feature extraction but accuracy is low [9].Panayiotis, Korfiatis gives brief information about an automated scheme for Texture-based identification and characterization of interstitial pheumonia patterns in lung multidetector CT. This method has high Feature extraction because it uses 3-d gray level cooccurrence features, stepwise discriminant analysis (SDA),K-NN classifier. But this method has high computational time [10]. Markus B. Huber1, Mahesh Nagarajan proposed that classification of interstitial Lung Disease Patterns with Topological Texture Features using k-Nearest Neighbor, Multilayer Radial Basis Function Neural Network for better classification performance but high computational complexity [11]. Lauge Sorensen, Saher B. Shake aims at improving quantitative measures of emphysema in computed tomography (CT) images of the lungs. Local binary patterns (LBP) are used as texture features, and joint LBP and intensity histograms are used for characterizing regions of interest (ROIs).Classification is then performed using a nearest neighbor classifier with a histogram dissimilarity measure as distance. It has good classification performance, with an accuracy of 95.2%.But feature extraction is low [12]. Daniel Sage, Asmaa Hidki describes a texture classification system that identifies lung tissue patterns from high resolution computed tomography images of patients affected with interstitial lung diseases (ILD). This pattern recognition task is part of an image–based diagnostic aid system for ILDs. Five lung tissue patterns selected from a multimedia database are classified using the discrete wavelet frame decomposition combined with grey–level histogram features. This method has high accuracy but the main weaknesses of the presented technique are the lack of resolution in scales with the DWF decomposition [13]. Ingrid Sluimer, Arnold Schilham presents a review of the literature on computer analysis of the lungs in CT scans and addresses segmentation of various

pulmonary structures, registration of chest scans, and applications aimed at detection, classification and quantification of chest abnormalities. Linear classifier, bayesian classifier are used for classification to increase the accuracy but it takes more time for computational [14] .Rahil Garnavi1, Ahmad Baraani aim to develop an accurate and reliable method for segmentation of lung HRCT images using a pixel based approach. This method combines traditional concepts such as global threshold segmentation, mathematical morphology, edge detection and noise reduction with new ideas, such as performing geometrical computations. Global threshold segmentation, edge detection this two methods are used. It has high feature extraction but classification rate is low [15].
Kwang Gi Kim, MS Jin Mo Goo develops an automated scheme to facilitate detection of localized ground-glass opacity (GGO) in the lung at computed tomography (CT). Here artificial neural network is used for fast classification but accuracy is low [16].

3. Proposed Work

In this work, we propose a new image classification method for lung tissue.
In this work, we propose a new image classification method for lung tissue patterns, based on feature-based image patch approximation.
A set of texture, intensity, and gradient (T-I-G) features are extracted for each image patch, and two new feature descriptors are proposed: 1) a new rotation-invariant Gabor-LBP (RGLBP) feature descriptor to represent rich texture features integrating multi-scale Gabor filters and LBP histograms; 2) a new multi-coordinate HOG (MCHOG) descriptor to extract the gradient features while accommodating rotation variance with radial-specific coordinate systems.
Each image patch is then classified using new patch-adaptive sparse approximation (PASA) algorithm, designed for better classification accuracy in the sparse representation.
Furthermore, since our proposed feature descriptors (RGLBP and MCHOG) and the approximative image classification algorithm (PASA) are designed based on few assumptions about the problem domain, these methods are thus extensible to other medical imaging problems as well.

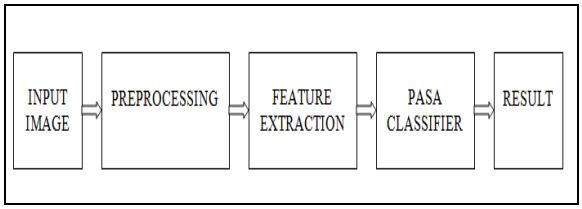

Figure 2: Block Diagram

3.1. Input Image

Input image is taken as gray level image. Because it has few levels (0-255) compared to RGB image.
In photography and computing, gray level digital image is an image in which the value of each pixel is a single sample, that is, it carries only intensity information. Images of this sort, also known as black-and-white, are composed exclusively of shades of gray, varying from black at the weakest intensity to white at the strongest.
Grayscale images are distinct from one-bit bi-tonal black-and-white images, which in the context of computer imaging are images with only the two colors black, and white (also called bi-level or binary images). Grayscale images have many shades of gray in between. Grayscale images are also called monochromatic, denoting the presence of only one (mono) color (chrome).
Grayscale images are often the result of measuring the intensity of light at each pixel in a single band of the electromagnetic spectrum (e.g. infrared, light, ultraviolet, etc.), and in such cases they are monochromatic proper when only given frequency is captured. But also they can be synthesized from a full color image; see the section about converting to grayscale.

3.2. Preprocessing

Preprocessing step is used to remove the noise..They are,

- Erosion
- Median filter
- Dilation
- Edge detection

3.2.1. Erosion

Two very common morphology operators are Dilation and Erosion. A set of operations that process images based on shapes. Morphological operations apply to an input image and generate an output image.
At each translated location, the structuring element values are subtracted from the image pixel values and the minimum is computed. The basic effect of the operator on a binary image is to erode away the boundaries of regions of foreground pixels (*i.e.* white pixels,

typically). Thus areas of foreground pixels shrink in size, and holes within those areas become larger.The erosion operator takes two pieces of data as inputs. The first is the image which is to be eroded. The second is a (usually small) set of coordinate points known as a structuring element (also known as a kernel).The structuring element that determines the precise effect of the erosion on the input image. To compute the erosion of a binary input image by this structuring element, consider each of the foreground pixels in the input image. For each foreground pixel (input pixel) superimpose the structuring element on top of the input image so that the origin of the structuring element coincides with the input pixel coordinates. If for every pixel in the structuring element, the corresponding pixel in the image underneath is a foreground pixel, then the input pixel is left as it is.

3.2.2. Median Filter

In signal processing, it is often desirable to be able to perform some kind of noise reduction on an image or signal. The median filter is a nonlinear digital filtering technique, often used to remove noise. Such noise reduction is a typical pre-processing step to improve the results of later processing (for example, edge detection on an image). Median filtering is very widely used in digital image processing because, under certain conditions, it preserves edges while removing noise. Median filtering is one kind of smoothing technique, as is linear Gaussian filtering. All smoothing techniques are effective at removing noise in smooth patches or smooth regions of a signal, but adversely affect edges. Often though, at the same time as reducing the noise in a signal,
it is important to preserve the edges. Edges are of critical importance to the visual appearance of images, for example. For small to moderate levels of (Gaussian) noise, the median filter is demonstrably better than Gaussian blur at removing noise. However, its performance is not that much better than Gaussian blur for high levels of noise, whereas, for speckle noise and salt and pepper noise (impulsive noise), it is particularly effective. Because of this, median filtering is very widely used in image processing.

3.2.3. Dilation

Dilation is the dual of erosion. At each translated location, the structuring element values are subtracted from the image pixel values and the minimum is computed. The basic effect of the operator on a binary image is to gradually enlarge the boundaries of regions of foreground pixels (*i.e.* white pixels, typically). Thus areas of foreground pixels grow in size while holes within those regions become smaller. The dilation operator takes two pieces of data as inputs. The first is the image which is to be dilated. The second is a usually small set of coordinate points known as a structuring element also known as a kernel. It is this structuring element that determines the precise effect of the dilation of the input image.

3.2.4. Edge Detection

The Sobel operator is used in image processing, particularly within edge detection algorithms. Technically, it is a discrete differentiation operator, computing an approximation of the gradient of the image intensity function. At each point in the image, the result of the Sobel operator is either the corresponding gradient vector or the norm of this vector. The Sobel operator is based on convolving the image with a small, separable, and integer valued filter in horizontal and vertical direction and is therefore relatively inexpensive in terms of computations.

3.3 Feature Extraction

In feature extraction first full lung images are taken. RGLBP and MCHOG are applied to full lung images for texture feature and gradient feature extraction. Then this image is cropped and given as name using PASA. Based on our visual analysis of lung images, it is observed that texture, intensity and gradient distribution of soft tissues within an image patch are quite informative and discriminative for different categories of lung tissues. Therefore, a patch-wise feature set, combining texture and gradient features are extracted for each image patch. And motivated by the recent works in the general imaging domain, we design a set of features based on the popular LBP and HOG descriptors, with modifications introduced for better feature descriptiveness. Formally, denote an image patch as comprising of X * Y Pixels P= {p_i:i=1,…,X*Y} , and I_i as the intensity value of pixel . The pixelp_i is also indicated by its coordinate as $p(x, y)$, and I(x, y)

3.3.1. Texture Description

The LBP feature describes the spatial structure of local image texture, and can be easily configured to be multi-resolution and rotation-invariant. However, the LBP feature might capture too many image details, and introduce large degree of unnecessary feature variations within the same tissue category. On the other hand, the multi-scale and multi-orientation representation of Gabor filters is often demonstrated as a highly effective texture descriptor. However, being rotation-variant, the Gabor filters become not directly suitable for our problem; but the multi-scale nature is quite useful for computing multi-resolution LBP features. Therefore, to incorporate rich texture information while attempting to minimize intra-category variations, we choose to design a new *rotation-invariant Gabor-LBP* (RGLBP) texture descriptor to incorporate the multi-scale property of Gabor filters and the rotation-invariant property of LBP features. Let $g_{s,r}(x, y)$represent the Gabor functions constructed from the basis function $g(x, y)$, with s=0, S-1and r=0, R-1 , where S and R denote the numbers of scales and orientations. The scale and orientation definitions follow the standard

conventions. A set of Gabor-filtered images $\{I^{s,r}\}$ are then computed by convolving image I with each Gabor function. To create rotation-invariant Gabor-filtered images, all R Gabor functions of a certain scale are summed together.

$I^s(x,y)=\sum_{r=0}^{R-1} I^{s,r}(x,y)$

The resultant image set thus comprises of only Gabor-filtered images $\{I^s = s = 0,...,$S-1$\}$, rather than the original set of S*R images, representing an -dimensional multi-scale and rotation-invariant texture feature for each pixel$P(x,y)$.

Next, for each Gabor-filtered image I^s,rotation-invariant LBP1 feature $LBP_s(p_i)$ is computed for each pixelp_i.

$LBP_s(p_i)$=min{ROR{$LBP'_s(p_i|8,1)$,n)

$LBP'_s(p_i|8,1)=\sum_n 1(I_i^s>I^s_{neigh(in)})2^n$

Where I_i^s denotes the intensity of pixel p_i in imageI^s, neigh (i,n) indexes the neighboring pixels (equally spaced on a circle of radius 1) of the center pixel n=0,..7, and .The operator ROR (.) performs a circular bit-wise shift to produce a minimum 8-bit number $LBP_s(p_i)$ and hence the LBP feature becomes rotation-invariant. Here, we simply use the eight immediate neighbors for calculating LBP, since the multi-resolution information is encoded in the Gabor-filtered images $\{I^s\}$.

The LBP features $LBP_s(p_i)$ of all pixels in the image patch P are then accumulated as a histogram feature $RGLBP_s$(p). As explained in [32], the total number of possible LBP values is 36, and hence the histogram $RGLBP_s$(p) of these pixel-wise LBP features is also 36-dimensional. And the concatenation of such histogram features from all scales $\{I^s\}$ is thus the final feature vector

RGLBP (P) = { $RGLBP_s$(p): s=0, S-1}

3.3.2. Gradient Description

Gradient distribution of an image is a different type of feature in complementary to the texture and intensity features. It is potentially very useful for discriminating pathological and normal lung tissues, since the former type often contains small segments that are less common in the normal lung. Among the various types of gradient-based features, the HOG feature has been suggested as very effective, especially when coupled with LBP features.

A problem with HOG features for lung images is, however, that it represents the distribution of absolute gradient orientations and hence is not invariant to rotations. While normally the rotation issue is tackled by assigning a dominant orientation based on local image statistics, such as SIFT .It is rather not intuitive to perceive a dominant orientation for image patches with complex textures. Therefore, inspired by the work on a SIFT-related rotation-invariant descriptor ,we design a new *multi-coordinate HOG* (MCHOG) descriptor to accommodate the possible rotations. The essential thought behind the Histogram of Oriented Gradient descriptors is that local object appearance and shape within an image can be described by the distribution of intensity gradients or edge directions. The implementation of these descriptors can be achieved by dividing the image into small connected regions, called cells, and for each cell compiling a histogram of gradient directions or edge orientations for the pixels within the cell.

The combination of these histograms then represents the descriptor. For improved accuracy, the local histograms can be contrast-normalized by calculating a measure of the intensity across a larger region of the image, called a block, and then using this value to normalize all cells within the block. This normalization results in better invariance to changes in illumination or shadowing.

Specifically, first, we denote the center pixel of image patch P as p_O . With as the origin, P is divided into V=8 radial sections, with the first section covering $[\pi/8,3\pi/8]$, and the rest covering the subsequent angle ranges. The image patch P can be thus represented by

$$P=\{RS_v(\alpha_{v,1},\alpha_{v,2}):v=1,\ldots V\}$$

$$\alpha_{v,1}=2v\frac{\pi}{V}-\frac{\pi}{V}$$

$$\alpha_{v,2}=2v\frac{\pi}{V}+\frac{\pi}{V}$$

And for each radial section RS_v, a coordinate system is defined

$$y_v=(1,\ll \alpha_{v,1}/2+\alpha_{v,2}/2)$$

$$x_v=\perp y_v$$

3.4. Approximate Patch Classification

The next step is to classify each image patch into one of the five tissue categories. Considering that lung images normally exhibit quite different patterns even within the same tissue category, we expect that even with the comprehensive feature design, large intra class variations would still exist. Therefore, we would like to use a classification scheme that is especially effective in handling such issues. And we thus design a data-adaptive and non- parametric approach, namely the *patch-adaptive sparse approximation* (PASA) method, to classify an image patch based on the closeness of approximation by other image patches from each tissue category. Denoting the five tissue categories normal T_N,emphysemaT_E,ground glassT_G, fibrosisT_F, and micro nodule T_M the objective here is to assign each image patch P a category label L(P) ϵ {$T_N T_E T_G T_F T_M$}.PASA method are described in the following

Assume that there are Q image patches belonging to a certain tissue category l ϵ {$T_N T_E T_G T_F T_M$ } in the training set. Denote this set of reference image patches as $\{P_q : q = 1, \ldots, Q\}$.An over complete feature dictionary matrix D_l for the Q reference image patches is then constructed by concatenating their features as column vectors

D_l={f(P_q): $q = 1, \ldots, Q$}$\epsilon R^{H \times Q}$

Where H is the feature dimension and H<Q , and each column vector f(p_q) is referred to as an atom. Here, five dictionaries are created with one for each tissue category, and the number of atoms in each dictionary could be different depending on the size of training data.

To classify an image patch, a sparse-regularized linear model is formulated to compute an approximated vector $f_l'(P)$ of its feature f(P) from the feature dictionary D_l

w_l=argmin|| f(P)-D_l w_l ||² s.t.|| w_l||≤C

$f_l'(P) = D_l w_l$

Where $w_l \epsilon R^{Q \times 1}$ is a sparse coefficient vector with nonzero elements, and C is a constant. Then, by deriving the feature approximation for each tissue category, the labeling L(P) of image patch (P) is the one producing the minimum discrepancy between the original feature f(P) and the approximated ones $\{f_l'(P)\}$.

L (P)=argmin|| f(P)- $f_l'(P)$ ||σ(w_l)

4. Implementation

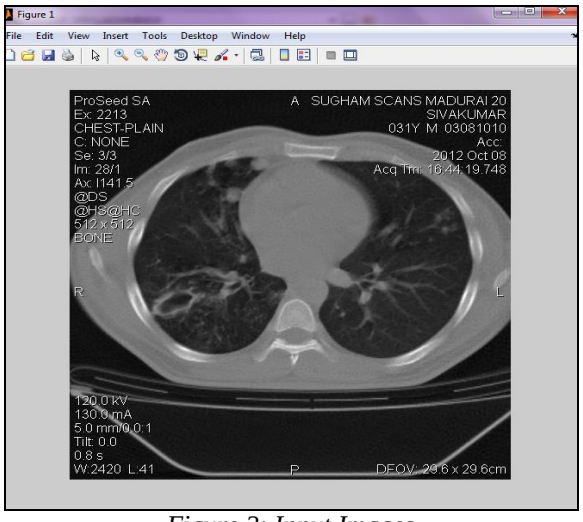

Figure 2: Input Images

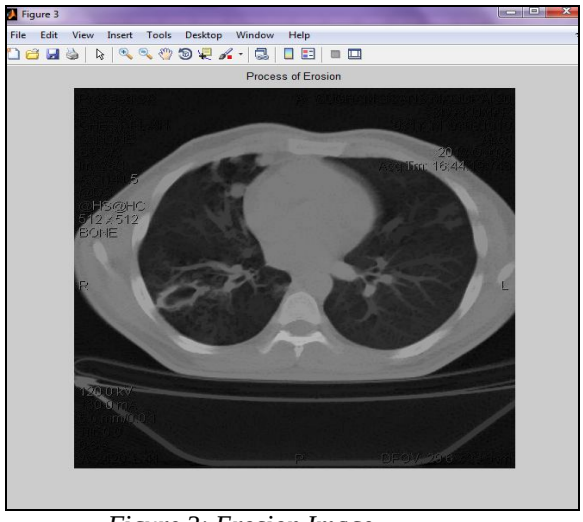

Figure 3: Erosion Image

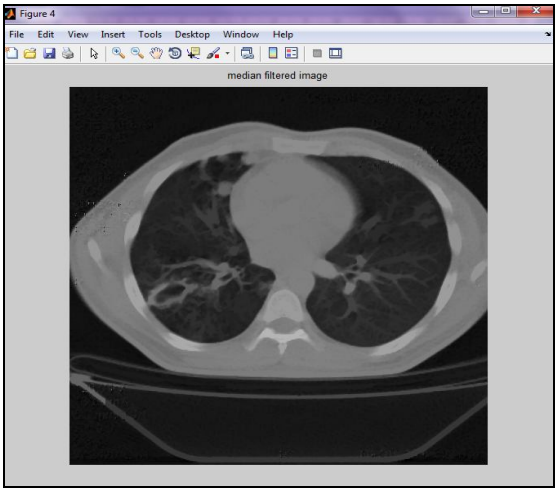

Figure 4: Median Filter Image

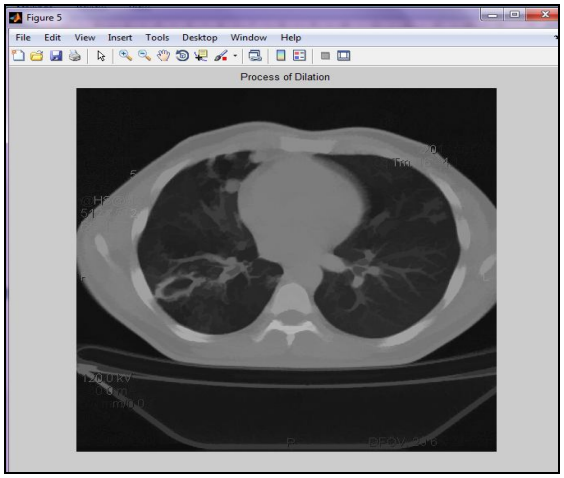

Figure 5: Dilation Image

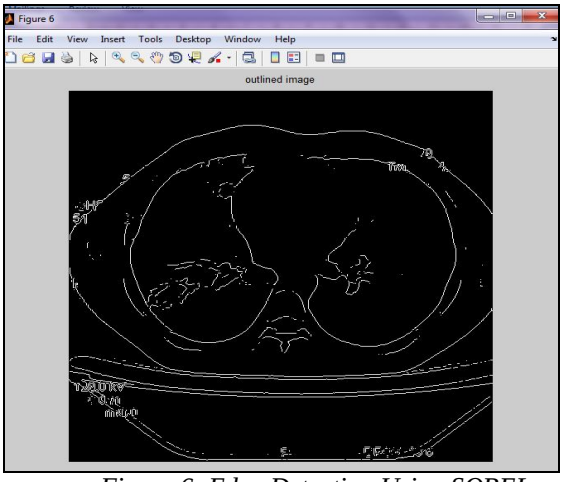

Figure 6: Edge Detection Using SOBEL

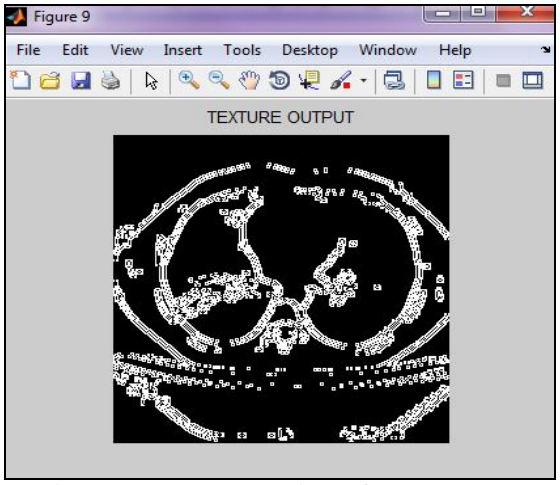

Figure 7: Texture Descriptor Output

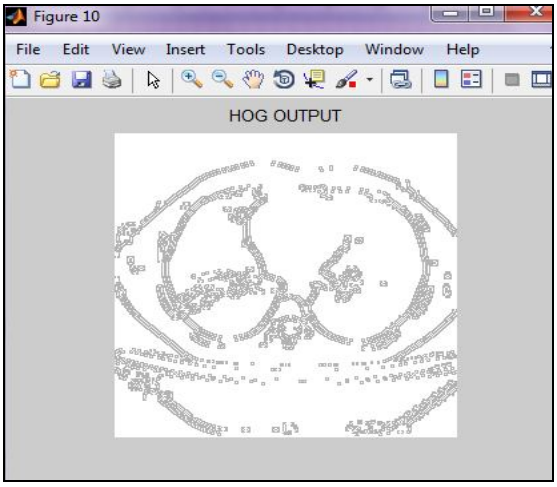

Figure 8: Gradient Descriptor Output

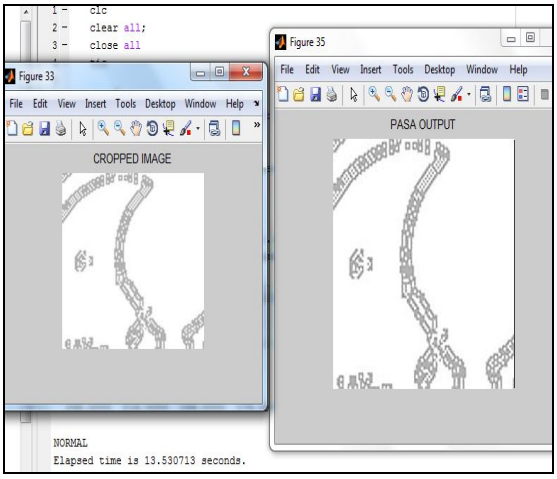

Figure 9: Normal Lung Tissue

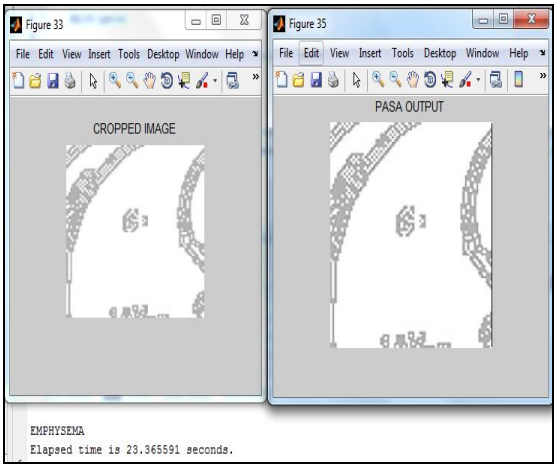

Figure 10: Emphysema Lung Tissues

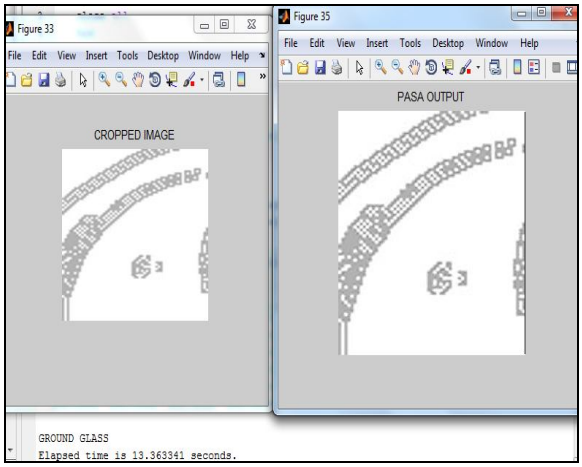

Figure 11: Ground Glass Lung Tissues

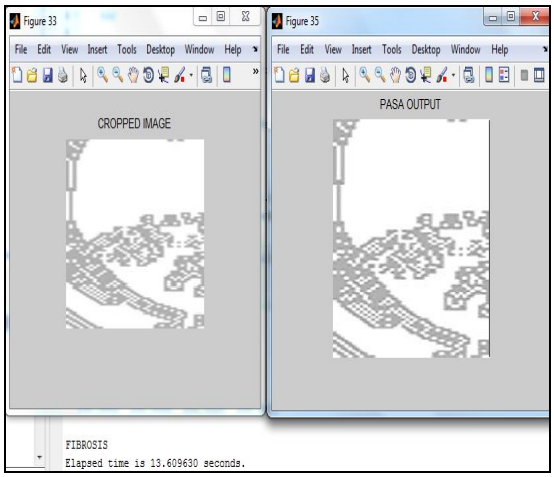

Figure 12: Fibrosis Lung Tissue

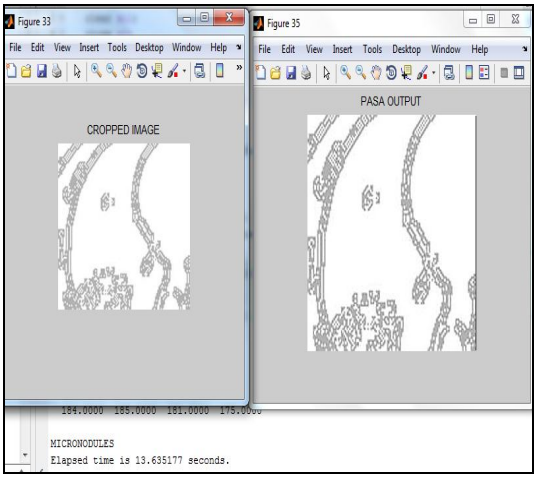

Figure 13: Micro Nodules Lung Tissue

5. Conclusion

An automatic classification method for lung HRCT images is presented in this paper. Five categories of lung tissues – normal, emphysema, ground glass, fibrosis and micro nodules—that are important for ILD disease diagnosis, are the main objects to be differentiated. To tackle the challenges in low inter-class distinctions and high intra-class variations, we have designed a feature-$T_E$based image patch approximation method. First, an image patch is represented as a feature vector, based on our proposed RGLBP texture and MCHOG gradient descriptors. Then, the image patch is classified into one of the five tissue categories, using our proposed PASA classifier based on reference image patches.

6. References

1. Yang song, Weidong cai,david dagan feng, " Feature-Based Image Patch Approximation for Lung Tissue Classification" IEEE transactions on medical imaging, vol. 32, no. 4, april 2013
2. Zhengyi Yang, Jeiran Choupan, Farshid Sepehrband, "Tissue Classification for PET/MRI Attenuation Correction Using Conditional Random Field and Image Fusion" International journal of machine learning and computing, vol.3, NO .1 feburary 2013.
3. S.Sivakumar, Dr.C.Chandrasekar, "Lung Nodule Detection Using Fuzzy Clustering and Support Vector Machines" International Journal of Engineering and Technology, Mar 2013.
4. Anam Tariq , M.usman Akram, "Lung Nodule Detection in CT Images using Neuro Fuzzy Classifier" TELKOMNIKA, Vol.11, No.2, June 2013.
5. A. Depeursinge, D. V. de Ville, A. Platon, A. Geissbuhler, P. A. Poletti, and H. Muller, "Near-affine-invariant texture learning for lung tissue analysis using isotropic wavelet frames," IEEE Trans. Inf. Technol. Biomed., vol. 16, no. 4, pp. 665–675, Jul. 2012.

6. U. Bagci, J. Yao, A. Wu, J. Caban, T. N. Palmore, A. F. Suffredini,O. Aras, and D. J. Mollura, "Automatic detection and quantification of tree-in-bud (TIB) opacities from CT scans," IEEE Trans. Biomed.Eng., vol. 59, no. 6, pp. 1620–1632, Jun. 2012.
7. V.Kumar, S.Jeyanthi ," Vascular Segmentation of Interstitial Pneumonia Patterns in Lung using MDCT", International Journal of Computer Science and Information Technology & Security (IJCSITS), ISSN: 2249-9555
   Vol. 2, No. 1, 2012.
8. QiSong,Milan Sonka, "Segmentation of pathological and diseased lung tissue in CT images using a graph-search algorithm" IEEE Trans. Med. Imag., vol. 29, pp. 2023–2037, March 2011.
9. Jianhua Yao, PhD1, Andrew Dwyer, "Computer-aided diagnosis of pulmonary infections using texture analysis and support vector machine Classification" NIH Public Access Author Manuscript Acad Radiol.2011 March; 18(3): 306–314. doi:10.1016/j.acra.2010.11.013.
10. P.D. Korfiatis, A.N. Karahaliou, A. D. Kazantzi, and L.I.Costaridou, "Texture-based identification and characterization of interstitial pheumonia patterns in lung multidetector CT," IEEE Trans. Inf. Technol. Biomed., vol. 14, no. 3, pp. 675–680, May 2010
11. Markus B. Huber1, Mahesh Nagarajan ," Classification of Interstitial Lung Disease Patterns with Topological Texture Features" arXiv:1005.5086v1 [physics.med-ph] 27 May 2010.
12. L.Sorensen, S. B. Shaker, and M. de Bruijne, "Quantitative analysis of pulmonary emphysema using local binary patterns," IEEE Trans. Med.Imag., vol. 29, no. 2, pp. 559–569, Feb. 2010.
13. Daniel Sage, Asmaa Hidki, "Lung Tissue Classification Using Wavelet Frames" 29th Annual International Conference of the IEEE EMBS Cité Internationale, France August 23-26, 2007.
14. I.Sluimer, A. Schilham, M. Prokop, and B. van Ginneken, "Computer analysis of computed tomography scans of the lung: A survey," IEEE
    Trans. Med. Imag., vol. 25, no. 4, pp. 385–405, Apr. 2006.
15. Rahil Garnavi1, Ahmad Baraani ,"A New Segmentation Method for Lung HRCT Images" Proceedings of the Digital Imaging Computing: Techniques and Applications 0-7695-2467-2/05 $20.00 © 2005 IEEE.
16. Kwang Gi Kim, MS Jin Mo Goo, MD, " Computer-aided Diagnosis of Localized Ground-Glass Opacity in the Lung at CT:Initial Experience"